29th International Cosmic Ray Conference Pune (2005) **00**, 101–104

Detecting Ultra High Energy Muons In Iron Calorimeter Detectors

Raj Gandhi[a], Sukanta Panda[a]
(a) Harish-Chandra Research Institute, India.
Presenter: Sukanta Panda( ),ind-panda-S-abs1-he21-oral

The origin of the knee in the energy spectrum of cosmic rays is still an unresolved problem. It arises because of the change in the slope of cosmic ray energy spectrum at the energy $(4-7)\times 10^{15}eV$. Existing detectors are insensitive to energies of secondary muons, allowing for the possibility that there which there may be missing energy carried away by the undetected particles produced at the knee. We model the cosmic ray muon flux above the knee by invoking new physics without relying on any specific model. With a large mass iron calorimeter(ICAL) detector one would be able to measure the energies of these muons using the pair meter technique. We estimate the event rates of muons in such a detector which would signal new physics, the number of interactions and their energy distribution, taking into account the effect of surrounding rock.

1. Introduction

Cosmic rays are observed in a wide range of energies. Energy of the cosmic rays ranges from eV to $10^{20}eV$. The energy spectrum of cosmic rays obeys a power law over a many order of magnitude. This power law behaviour breaks at the knee which occurs at energy $\simeq 4\times 10^{15}eV$ and again at the ankle which occurs at energy $\simeq 5\times 10^{18}eV$. Let's consider the differential flux $dN/dE\sim E^{-\alpha}$. α takes value 2.7 untill knee. After the knee α changes to 3.1. This change in the slope of the cosmic ray spectrum at the knee is not clearly understood so far because above the knee energy, energy resolution of the ground array experiments is very poor.

Interaction of high energetic primary cosmic rays with the air nuclei in the atmosphere develops extensive air shower with electromagnetic, hadronic and deeply penetrating muon component. Basically energy of primary particles is distributed among these components. In most of the ground array experiments we measure number of secondary particle produced such as electrons, muons etc but not the energy. The knee problem can be solved in two ways. First way is to consider a change in the composition of the primary cosmic ray flux near knee energy. Second way may be the creation of new heavy particles at knee energy. For a review of several models, we refer the reader to [1]. Here we will concentrate on the second case. For the measurement of energy of muon we use pair meter technique. This technique is useful only when we have large-scale iron calorimeter detectors. Previous designed detectors are failed so far to make this technique fruitful because of their small size. Future Indian neutrino observatory(INO) experiments will be able to measure energy of muons more accurately.

The advantages of pair meter technique is that energy resolution is not deterioated with the increase in muon energy.

2. Interaction of Muons With Matter

A better understanding of muon energy loss in any medium at high energies is required for the energy measurement. Muon loses it's energy through ionization, bremsstrahlung, pair production and photonuclear scattering at high energies. The direct production of electron-positron pairs dominate other processes at low energy transfers and complete screening [2, 3].

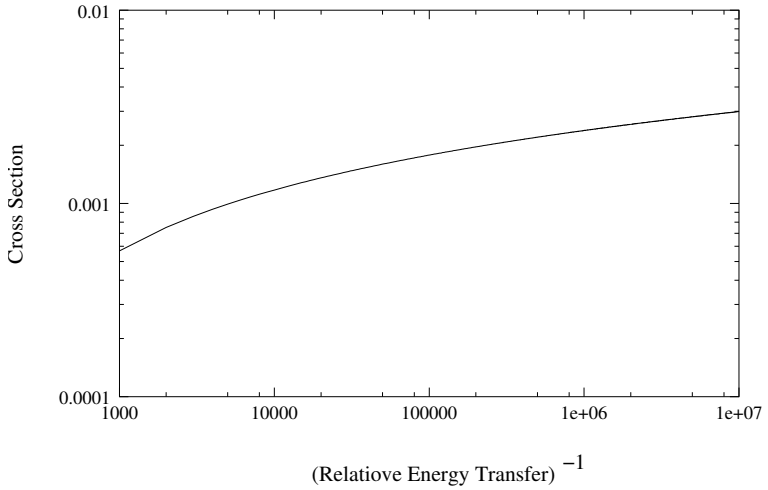

Figure 1. Differential cross section $\epsilon\sigma_d(E,\epsilon)$ vs. E/ϵ (inverse of the relative energy transfer)

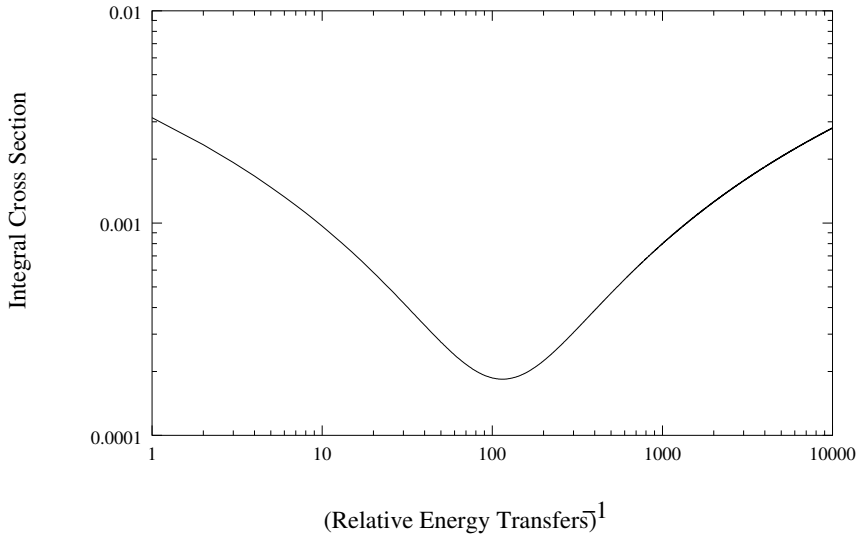

Figure 2. Integral Cross Section $\sigma_i(E,\epsilon)$ vs. E/ϵ (inverse of relative energy transfer)

In the approximation, $\frac{\epsilon}{E} \ll \frac{2m_e}{m_\mu}$ and $\epsilon \gg 2m_e 189\sqrt{e}Z^{-1/3} \simeq 0.3Z^{-1/3}GeV$, differential pair production is given by

$$\epsilon\sigma_d(E,\epsilon) \simeq \frac{14\alpha}{9\pi t_0} ln\left(\frac{\kappa m_e E}{\epsilon m_\mu}\right) , \tag{1}$$

where ϵ is the energy tranfer, E is the muon energy, m_e is the mass of electron, m_μ is the mass of muon, $\alpha = 1/137$, $\kappa \simeq 1.8$ and t_0 is the radiation lenth (r.l) which is

$$t_0 = \left(\frac{4Z(Z+1)}{A}\,\alpha r_0^2 N_0\, ln(189Z^{-1/3})\right)^{-1} , \tag{2}$$

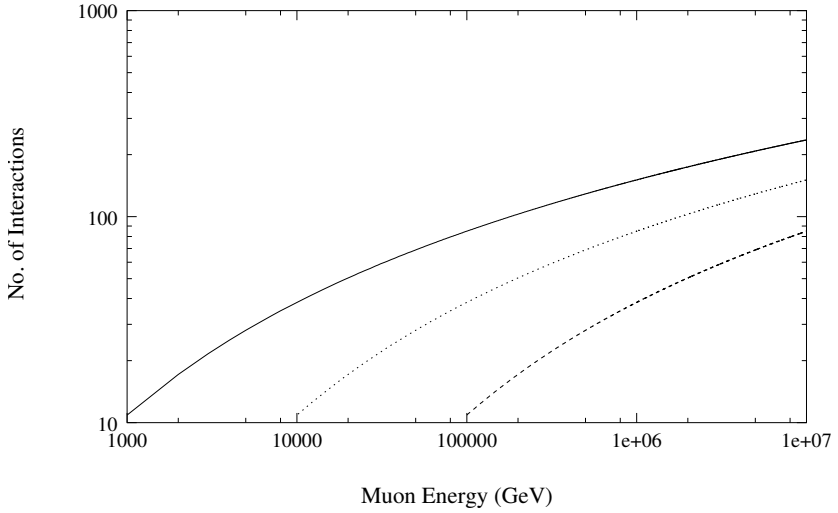

Figure 3. Number of interactions vs. muon energy for $\epsilon_0 = 1GeV(solidline), 10GeV(dotted), 100GeV(dashed)$ while T is fixed to 1000 r.l.

where A is the atomic weight, r_0 is the classical radius, N_0 is the Avagadro number and Z is the atomic number. The behaviour of differential cross section with inverse of relative energy transfer is given in fig. 1.

Similarly we can write the integral cross section with energy transfer above some threshold ϵ_0. If $\epsilon_0 \leq 10^{-3}E$ then the integral pair production cross section is given by,

$$\sigma_i(E,\epsilon) \simeq \frac{7\alpha}{9\pi t_0}\left(ln^2\left(\frac{\kappa m_e E}{\epsilon_0 m_\mu}\right) + C\right) \ , \tag{3}$$

where $C \simeq 1.4.$‘ The cross section is plotted in fig. 2.

2.1 Muon loss at a depth X

At muon energies $E_\mu \geq 1TeV$, the average loss almost increases linearly with energy which satisfies a relation,

$$\left\langle \frac{dE}{dX} \right\rangle = -\alpha - \beta E \ , \tag{4}$$

where α gets contribution from ionization of muons and β gets contribution from bremsstrahlung, pair production and photonuclear process. Assuming α and β does not change with energy, we get average muon energy at depth X as

$$\langle E(X) \rangle = \left(E_0 + \frac{\alpha}{\beta}\right) e^{-\beta X} - \frac{\alpha}{\beta} \ , \tag{5}$$

where E_0 is the initial muon energy. Minimum energy required of a muon at the surface reach depth X is give by,

$$E_0^{min} = \frac{\alpha}{\beta}\left(e^{\beta X} - 1\right) \ . \tag{6}$$

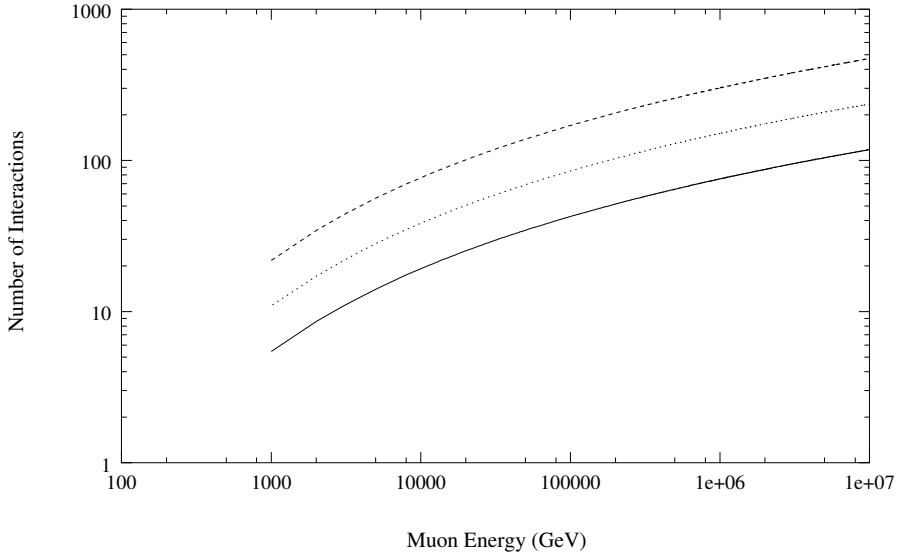

Figure 4. Number of interactions vs. muon energy for $T = 500(dashedline), 1000(dotted), 2000r.l(solidline)$ while ϵ_0 is fixed to 1 GeV.

¿From Eq. 5, we get the relation between initial energy E_0 and degarded energy of muon E_μ after travelling a distance X as,

$$E_0 = \left(E_\mu + \frac{\alpha}{\beta}\right) e^{\beta X} - \frac{\alpha}{\beta} \,. \tag{7}$$

Differential muon flux at a depth X is given by,

$$\frac{dN}{dE_\mu} = \frac{dN}{dE_0} e^{\beta X} \,. \tag{8}$$

where $\frac{dN}{dE_0}$ is the initial muon flux with energy E_0.

In ref. [4], it is shown that α and β value in the analytical expression can be obtained for standard rock, in the depth range $(4-10) \times 10^5 g/cm^2$. The values are,

$$\beta = 3.74 \times 10^{-6} cm^2/g, \; \frac{\alpha}{\beta} = 647 GeV. \tag{9}$$

For these values of α and β, the analytical expression for the muon flux at depth X matches well with monte carlo results done in ref. [4].

3. Energy Estimation and Number of Interactions

Authors of ref. [3] have evaluated expressions for energy, number of interaction and energy measurement errors in pair meter theory. We outline here their results. We take the simplest case where number of interaction obeys a poisson distribution. The expression for number of interactions M and energy E for the threshold energy region $\epsilon_0 \leq 10^{-3} E$ is given by,

$$M = \frac{7\alpha T}{9\pi} \left(ln^2 \left(\frac{\kappa m_e E}{m_\mu \epsilon_0} \right) + C \right) \,, \tag{10}$$

$$E = \frac{m_\mu \epsilon_0}{\kappa m_e} \exp\left(\sqrt{\frac{9\pi M}{7\alpha T} - C}\right) . \tag{11}$$

where T is the thickness of the material in units of r.l. The behaviour of M with energy is shown in fig. 3 for different energy transfers ϵ_0 and in fig. 4 for different thick nesses of the apparatus. We can clearly seen from Table. 1 that number of interaction increases as the energy of muons increases.

$E_\mu(TeV)$	1	10	100	1000	10000
M	10.889	38.363	84.991	150.774	235.712

Table 1. No. of interactions at different muon energies for $\epsilon_0 = 1GeV$.

$E_\mu(TeV)$	Model no. 1	Model no. 2	Model no. 3
100	486	342	496
200	43	1424	122
300	11	1593	48
400	4	1384	24
500	2	1126	13
600	1	785	9
700	.5	602	5
800	.3	469	4
900	.2	371	3
1000	.1	298	2
10000	10^{-5}	0.6	.001

Table 2. Number of events in 3 years of exposure time for three different flux model. No degradation in energy of muons due to surrounding rock is taken into account.

4. Flux Model

Here we describe three flux models.

4.1 Model 1

Differential conventional muon fluxes from the decay of pion and muon decays[5] read as,

$$\frac{dN}{dE} = \frac{N_0 E^{-\gamma-1}}{1+AE} \tag{12}$$

for $E < E_0$.

$$\frac{dN}{dE} = \frac{N_0^{'} E^{-\gamma^{'}-1}}{1+AE} \tag{13}$$

for $E > E_0$. For conventional flux $N_0 = 0.2, N_0^{'} = 0.2, \gamma = 1.74, \gamma^{'} = 2.1, E_0 = 5.3 \times 10^5, A = 0.007$.

As we explained in the Introduction of this paper that we would be looking at a option for the explanation of cosmic ray knee in which new processes dominates the dynamics at the knee energy. In this option we assume

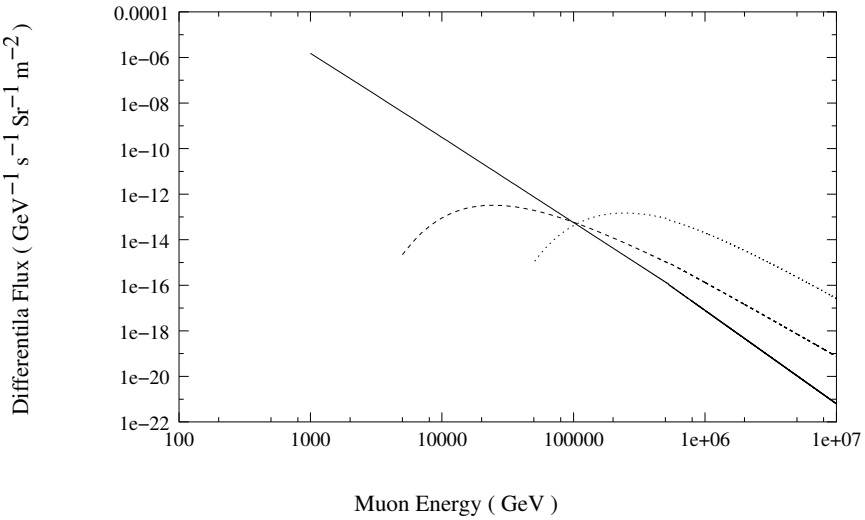

Figure 5. Differential flux vs. muon enegy for model 1(solid line), model 2(dotted line) and model 3(dashed line) respectively.

that some new particle of mass $\approx TeV$ are produced at knee because center of mass energy of the interaction of primary cosmic rays with the air nuclei at knee is of the order of TeV. This might be responsible for the change of the cosmic ray spectrum slope at knee.

We can calculate the missing energy by comparing the following two fluxes at knee energy E_0. Assumed two energy spectra with different exponent, we write

$$N_1 = N\left(\frac{E_0}{E_1}\right)^{\gamma_1} \tag{14}$$

and

$$N_2 = N\left(\frac{E_0}{E_2}\right)^{\gamma_2}, \tag{15}$$

where N is the particle density at knee energy. By comparing the Eq. 14 and Eq. 15, we get missing energy δE as

$$\delta E = E_1\left(1 - \left(\frac{E_0}{E_1}\right)^{\delta\gamma/\gamma_2}\right) \tag{16}$$

where $\delta E = E_1 - E_2$ and $\delta\gamma = \gamma_2 - \gamma_1$. For $E_0 = (4-7)\times 10^{15} eV = (4-7) PeV$, $\gamma_2 = 2.1$ and $\delta\gamma = 0.4$.

In order to explain the knee puzzle, this extra energy must be taken away by unobserved particles as we don't measure the energy in ground array experiments. In the framework of Standard Model(SM) the unobserved particles can be three neutrinos and muons. Among these particles muons can be detected with higher probability. To estimate the event rate of muons in Iron Calorimeter detectors we need to know the muon flux after including new processes at the knee. Here one searches for models beyond SM where one can accomodate such a scenario. Without knowing the details of the model here we calculate energy spectrum of muons by considering two limiting cases. Then any model lies in between these two limiting cases could be a reasonable model to solve the knee puzzle.

4.2 Model 2

In this case where three neutrinos and only one muon produced in the process then energy carried away by the muon is $\delta E/4$. Then muon flux looks like

$$dN/dE_\mu = 0.2 \times 10^4 \times e^{-5\times10^6/(4(E_\mu - E_1))} \frac{(E_\mu - E_1)^{(-1.74-1)}}{1 + 0.007(E_\mu - E_1)} \tag{17}$$

for $E_\mu < 5.3 \times 10^5 GeV$ and

$$dN/dE_\mu = 22 \times 10^4 \times e^{-5\times10^6/(4(E_\mu - E_1))} \frac{(E_\mu - E_1)^{(-2.1-1)}}{1 + 0.007(E_\mu - E_1)} \tag{18}$$

for $E_\mu > 5.3 \times 10^5 GeV$, where $E_1 = E_\mu \left(1 - \frac{5\times10^6}{4E_\mu}\right)^{0.4/2.1}$.

4.3 Model 3

In this case apart from three neutrinos, ten muons are produced in the process then energy carried away by the muon is $\delta E/40$. Then muon flux looks like

$$dN/dE_\mu = 0.8 \times e^{-5\times10^6/(40(E_\mu - E_2))} \frac{(E_\mu - E_2)^{(-1.74-1)}}{1 + 0.007(E_\mu - E_2)} \tag{19}$$

for $E_\mu < 5.3 \times 10^5 GeV$ and

$$dN/dE_\mu = 88 \times e^{-5\times10^6/(40(E_\mu - E_2))} \frac{(E_\mu - E_2)^{(-2.1-1)}}{1 + 0.007(E_\mu - E_2)} \tag{20}$$

for $E_\mu > 5.3 \times 10^5$, where $E_2 = E_\mu \left(1 - \frac{5\times10^6}{40E_\mu}\right)^{0.4/2.1}$.

For all cases fluxes are plotted in fig. 5.

5. Event Rate

Number of integral events in ICAL detectors can be expressed as

$$Eventrate = \int_{E_t h}^{\infty} \sigma_i(E, \epsilon_0) \frac{dN}{dE_\mu} \times \rho \times A \times T \times t \,, \tag{21}$$

where ρ is the density of the material, A is the area of the detector, T is the thickness of the detector and t is the exposure time. For INO ICAL detectors, we have taken $A = 4.5 \times 10^6 cm^2$, $A = 13.5 \times 10^6 cm^2$, $T = 1310 cm$ and $\rho = 7.87 g/cm^2 for steel$. This all amounts to 100 Kton ICAL detector.

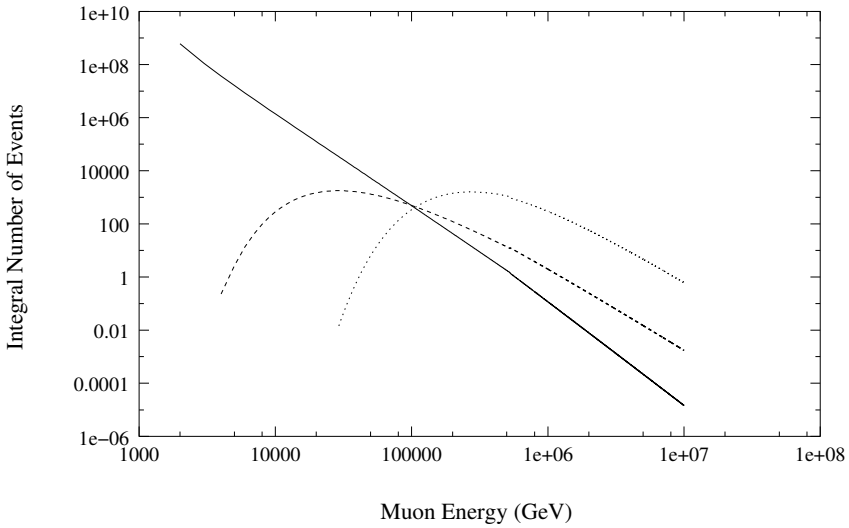

Figure 6. Number of events vs. muon energy for 100 KTon Ical detectors in 3 years of exposure time for flux model 1(solid line), model 2(dotted line) and model 3(dashed line). Here effect from surrounding rock is not taken into account.

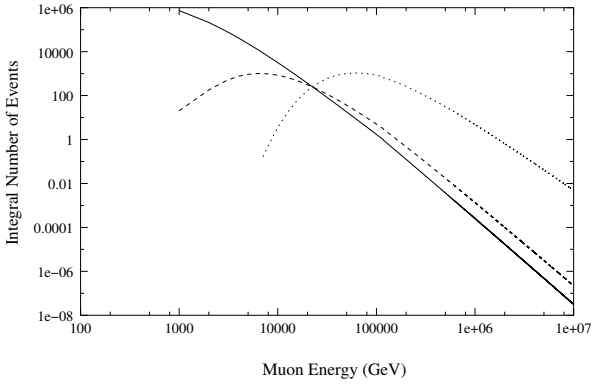

Figure 7. Number of events vs. muon energy for 100 KTon Ical detectors in 3 years of exposure time for flux model 1(solid line), model 2(dotted line) and model 3(dashed line). Here effect from surrounding rock is taken into account. Width of rock is taken to be $4 \times 10^5 g/cm^2$.

6. Discussion

Results of the event rate calculations for all three models are given in Fig. 6 and Fig. 7. We also tabulate our results in Table. 2 and 3. We can observe clearly thousand events for model 2 and hundred events for model 3 in three years of exposure time of the ICAL detectors. With the conventional flux (model 1) one can observe few hundred events in 3 years of exposure time of the ICAL detectors.

References

[1] Jorg R. Horandel, Astropart.Phys. **21**, 241 (2004) astro-ph/0402356

$E_\mu(TeV)$	Model no. 1	Model no. 2	Model no. 3
100	2	845	5
200	.1	260	.5
300	.02	109	.1
400	.008	54	.03
500	.003	31	.01
1000	.0002	5	.001
10000	10^{-8}	.0005	10^{-7}

Table 3. Number of events in 3 years of expossure time for three different flux models by taking into account the degradation in energy of muons while passing though the surrounding rock covering the detector.

[2] R. P. Kokoulin and A. A. Petrukhin, Sov. J. Part. Nucl **21**(3), 332 (1990).
[3] R. P. Kokoulin and A. A. Petrukhin, Nucl. Instrum. Methods Phys. Res. A **263**, 468 (1988).
[4] C. Castagnoli et. al, Phys. Rev. D **52**, 2673 (1995).
[5] M. Thunman, G.Ingelman, P. Gondolo, Astropart.Phys. **5** 309 (1995)